

AD-A149 959

MICROSTRUCTURAL AND ELECTRONIC CHARACTERISTICS OF  
METALLIC SPIN GLASSES. (U) SALFORD UNIV (ENGLAND) DEPT  
OF PURE AND APPLIED PHYSICS A J JANICKI ET AL.

1/1

UNCLASSIFIED

15 NOV 84 AFOSR-TR-84-1237 AFOSR-80-0005

F/G 11/2

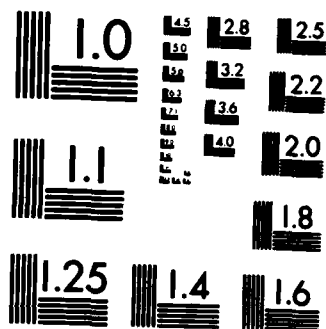
NL

END

FORMED

DTIC





MICROCOPY RESOLUTION TEST CHART  
NATIONAL BUREAU OF STANDARDS-1963-A

AFOSR-TR-84-1237

(3)

MICROSTRUCTURAL AND ELECTRONIC CHARACTERISTICS OF METALLIC SPIN GLASSES

A.J. Janicki and R.S. Tebble  
Department of Pure and Applied Physics  
University of Salford  
Salford M5 4WT  
England

15 November 1984

Final Scientific Report 1 October 1983 - 30 September 1984

Approved for public release; distribution unlimited.

Prepared for

AIR FORCE OFFICE OF SCIENTIFIC RESEARCH AND DEVELOPMENT/LNM

and

EUROPEAN OFFICE OF AEROSPACE RESEARCH AND DEVELOPMENT  
London, England.

AD-A149 959

DTIC FILE COPY

DTIC  
SELECTE  
FEB 7 1985  
D

Weinstock

REPORT DOCUMENTATION PAGE		READ INSTRUCTIONS BEFORE COMPLETING FORM	
1. Report Number AFOSR-TR-	2. Accession No. 2287 AD-A149959	3. Recipient's Catalog Number	
4. Title (and Subtitle) Microstructural and Electronic Characteristics of Metallic Spin Glasses		5. Type of Report & Period Covered Final Scientific Report 83 Oct 01 - 84 Sept 30	
		6. Performing Org. Report Number	
7. Author(s) A.J. Janicki and R.S. Tebble		8. Contract or Grant Number AFOSR 80-0005	
9. Performing Organization Name and Address University of Salford Department of Pure and Applied Physics Salfore M5 4WT, ENGLAND		10. Program Element, Project, Task Area & Work Unit Numbers <del>82-0223</del> 61102F, • 2306/C3	
11. Controlling Office Name and Address Air Force Office of Scientific Research Building 410 Bolling AFB. DC 20332		12. Report Date 15 November 1984	
		13. Number of Pages 18	
14. Monitoring Agency Name and Address European Office of Aerospace Research and Development/LNM Box 14 EPO New York 09510		15.	
16. & 17. Distribution Statement Approved for public release; distribution unlimited.			
18. Supplementary Notes			
19. Key Words Spin glasses, metallic glasses, magnetic clustering, Fe-Ni-B-Si, electron microscopy.			
20. Abstract In the report, the structural relaxation process of $\text{Fe}_{10}\text{Ni}_{65}\text{B}_{15}\text{Si}_{10}$ amorphous spin glass is described. The ribbon samples were prepared by melt spinning and heat treated using two different annealing processes AP1 and AP2. The techniques employed to investigate structural changes in the three alloy states AQ (as-quenched), AP1 and AP2 were as follow: transmission electron microscopy, scanning electron microscopy with X-ray analysis, differential scanning calorimetry and density determination. Differences were detected in the amorphous structures for two states of relaxation in the alloy. The formation of clusters is proposed for one alloy state and the influence of clustering on the early stages of crystallization is discussed.			

## ABSTRACT

In the paper the structural relaxation process of  $\text{Fe}_{10}\text{Ni}_{65}\text{B}_{15}\text{Si}_{10}$  amorphous spin glass is described.

The ribbon samples were prepared by melt spinning and heat treated using two different annealing processes AP1 and AP2.

The techniques employed to investigate structural changes in the three alloy states AQ (as-quenched), AP1 and AP2 were as follows: transmission electron microscopy, scanning electron microscopy with X-ray analysis, differential scanning calorimetry and density determination.

Differences were detected in the amorphous structures for two states of relaxation in the alloy. The formation of clusters is proposed for one alloy state and the influence of clustering on the early stages of crystallization is discussed.

Accession For	
NTIS GRA&I	<input checked="checked" type="checkbox"/>
DTIC TAB	<input type="checkbox"/>
Unannounced	<input type="checkbox"/>
Justification	<input type="checkbox"/>
Distribution/	
Availability Codes	
A-1	

AIR FORCE CORP  
KIRK

## 1. INTRODUCTION.

During recent years many papers have appeared dealing with spin glass alloys. Most of them investigated the magnetic properties and the nature of the origin of boundary lines around the multicritical point (MCP). Beck [1] and Tholence and Tournier [2] proposed that clusters of spins play an important role in the spin glasses. In their approach the alloy was treated as a composition of rigid moments frozen in by local anisotropy fields, however the microscopic origin was not described. Riess [3] and Larsen [4] introduced a fully dynamic description permitting a range of freedom of the clusters. Edwards and Anderson [5] proposed a model where the Heisenberg Hamiltonian describes the spin glass, and suggested that in a system of randomly oriented spins, a magnetic state with short-range order could occur. Sherrington and Kirkpatrick [6] proposed a model where the measure of ferromagnetic exchange couplings describes the distribution of exchange energy.

A rather original approach to the problem was made by Soukoulis and Levin [7] who proposed a cluster-mean-field theory (CMFT) of the spin glasses, suggesting that correlated clusters and not individual spins are the basic entity. In this model two variables were introduced the anisotropy field,  $q$ , and the cluster moment,  $M$ .

There is therefore, a direct correlation between  $M$  and the fluctuation effects as both are temperature dependant.

Levin (7) who proposed a cluster-mean-field theory (CMFT) of the spin glasses, suggesting that correlated clusters and not individual spins are the basic entity. In this model two variables were introduced the anisotropy field,  $q$ , and the cluster moment,  $M$ . There is therefore, a direct correlation between  $M$  and the fluctuation effects as both are temperature dependent.

Spin glass models are based on the assumption of an exchange interaction between a given atom and its near-neighbours. Therefore, it follows that any variation in atomic positions in the amorphous state will have a considerable effect on the exchange interaction.

We can assume that the magnetic properties such as static-zero-field susceptibility, ac-susceptibility, magnetic-specific-heat, Hall effect, Mössbauer splitting, as well as thermoelectric power and magnetoresistance are strongly dependent on the location of atoms in amorphous structure. Other factors of prime importance are cluster size and cluster density in the amorphous matrix. Therefore, structural relaxation and change in chemical-short-range order (CSRO) in amorphous spin glasses are closely linked with their magnetic nature.

There are a number of spin glass alloys that have been the subject of numerous investigations such as AuFe, CuMn, CoGa, FeZr,  $(\text{Fe}_{1-x}\text{Ni}_x)_{75}\text{B}_{15}\text{Si}_{10}$  as well as  $(\text{A}_x\text{B}_{1-x})_{75}\text{P}_{16}\text{B}_6\text{Al}_3$ , where  $A = \text{Fe, Co}$  and  $B = \text{Ni, Mn, Cr, Mo}$ . The subject of this investigation is the amorphous alloy  $\text{Fe}_{10}\text{Ni}_{65}\text{B}_{15}\text{Si}_{10}$ . In the paper we shall deal mainly with the relaxation process in the alloy, but reference is also made to ac-susceptibility measurements.



## 2. EXPERIMENTAL.

A metallic glass ribbon  $\text{Fe}_{10}\text{Ni}_{65}\text{B}_{15}\text{Si}_{10}$ , 8 mm wide and 30  $\mu\text{m}$  thick was produced by the melt spinning technique.

The amorphous state of the ribbon was determined by X-ray diffraction using  $\text{CuK}_\alpha$  radiation. Ribbon samples were heat treated in quartz ampules under high vacuum, using two different annealing processes; AP1: at 480 K for 200 min, and AP2: at 580 K for 400 min., and amorphous state was again confirmed.

Experiments were performed on AQ (as-quenched), AP1 and AP2 samples.

Thin foil microscope specimens were prepared using a Struers double side thinning apparatus and a JEOL 200 CX transmission electron microscope (TEM) was used to study morphology and the first stages of crystallization. A differential scanning calorimeter (DSC) Perkin-Elmer DSC-2 was employed to determine the onset of the crystallization temperatures,  $T_x$  and the activation energy for crystallization,  $E_a$ , calculated by Kissinger method. The microcalorimeter was calibrated to within  $\pm 1$  K with a sensitivity of 5 mcal  $\text{sec}^{-1}$ .

A bend test was carried out on an Instron testing machine with parallel plates, operating at a speed of 5 mm  $\text{min}^{-1}$  and a plot of interplates distance vs load was recorded.

Flat, 0.25  $\mu\text{m}$  diamond polished cross sections of AQ, AP1 and AP2 samples were examined and analysed using a Cambridge 604 scanning electron microscope (SEM) with a Link X-ray energy dispersive analyser.

Finally the changes in density were determined using Archimedes method with xylene as the liquid media and an Oertling balance with a tolerance of  $\pm 10^{-5}$  g.

### 3. RESULTS

The X-ray diffraction pattern of AQ  $\text{Fe}_{10}\text{Ni}_{65}\text{B}_{15}\text{Si}_{10}$  exhibits an amorphous structure over the entire ribbon, with an average d-distance of 1.98 Å.

#### 3.1 DSC Measurements

On Fig. 1 is shown a typical thermogram at heating rate of 20 K min<sup>-1</sup>. The values of  $T_x$  and  $E_a$  for AQ, AP1 and AP2 materials are listed in Table 1.

Table 1.  $T_x$ ,  $E_a$  for  $\text{Fe}_{10}\text{Ni}_{65}\text{B}_{15}\text{Si}_{10}$  in AQ, AP1 and AP2 state

$H_R$ K min <sup>-1</sup>	5	10	20	50	100	$E_{a1}$	$E_{a2}$
		$T_{x1}$	$T_{x2}$	/ K /		eV	
AQ	704,763	715,775	721,782	737,795	744,800	3.25	4.68
AP1	706,763	716,775	722,780	739,797	744,800	3.55	4.62
AP2	707,762	717,775	723,780	738,794	743,800	3.87	4.26

The effect of the first annealing process AP1 is to increase the  $T_{x1}$  temperatures, which may be clearly seen from results of the lower heating rates (HR), however, there is no noticeable change in the values of the  $T_{x2}$  temperatures. The second annealing process AP2 produces very little change in the value of the  $T_{x1}$  temperature and causes a slight decrease in the value of the  $T_{x2}$ .

The activation energy of the first stages of crystallization  $E_{a1}$  increased gradually for both AP1 and AP2 processes, while the  $E_{a2}$  remained unchanged. Further experiments were carried out on the SEM and TEM to investigate the rise in  $E_{a1}$  more closely.

### 3.2 Density and Embrittlement

The density of amorphous FeNiBSi spin glass increased upon both AP1 and AP2 annealings as is shown in Table 2.

State of alloy	AQ	AP1	AP2
Density g cm <sup>-3</sup>	7.638	7.712	7.729

The total change in density from the as-quenched to the annealed state is 1.2% which is higher than most of the reported data [8]. However, this may be explained by the large concentration of metalloid atoms in the metallic glass, and suggests the "soft sphere" model is applicable for this alloy. During the first annealing process (AP1) there is an increase in density which may be explained by the elimination of excess free volume, and this free volume decrease is associated with a change in topological short-range order (TSRO).

The calculated amorphous alloy packing fraction  $n_a$  increases with annealing and these values are 0.7266, 0.7336, 0.7352 for AQ, AP1 and AP2 respectively.

The recorded changes in ductility for samples AQ and AP1 are presented on Fig. 2, and for sample AP1 there is an increase in strain  $\epsilon_0$  corresponding to the onset of permanent deformation [9]. It should be noted that an increase in strain after the annealing process is indicative of changes in TSRO.

TEM, SEM and X-ray energy dispersive analysis were employed to identify the nature of structural changes in the amorphous state and their influence on the early stages of crystallization.

### 3.3 TEM

The in-situ early stages of crystallization were observed using a heating holder in the TEM and the estimated average heating rate was  $10 \text{ K min}^{-1}$ . Figs. 3 and 4 present crystallization sequences of AP1 and AP2 samples, respectively.

AP1 spin glass crystallized in four stages, as follows:

- I 300-520 K, the  $d$ -spacing of the amorphous phase ( $d_{AM}$ ) remain unchanged at  $2.075 \text{ \AA}$ .
- Ia 520-670 K, the value of  $d_{AM}$  increases to  $2.098 \text{ \AA}$ , however the alloy remains in the fully amorphous state (Fig. 3a).
- II 670-730 K, first crystals of spherulitical morphology appear, and the  $d_{AM}$  value remains as in stage Ia despite an increase in the degree of crystallinity and a rise in temperature (Fig. 3b,c).
- III annealing at 730 K for 15 min, results in a further increase in both crystal size and number,  $d_{AM}$  increases slightly to  $2.125 \text{ \AA}$  (Fig. 3 d,e) and there is a total decomposition of the amorphous phase.

The crystallization of AP2 material proceeded as follows:

- I 300-680 K, alloys remains fully amorphous with  $d_{AM} = 2.11 \text{ \AA}$  (Fig. 4a)
- II 680-740 K, microcrystals appear in large number and as crystallization progresses  $d_{AM}$  increases to  $2.15 \text{ \AA}$  (Fig. 4b)
- III 740 K, a fully decomposed amorphous phase, and a microcrystalline structure with polygonal morphology (Fig. 4 c,d).

The following differences in the crystallization between AP1 and AP2 specimens were observed:

- 1  $d_{AM}$  of AP2 material does not change until the onset of the crystallization, i.e. 680 K, but the  $d_{AM}$  of AP1 material starts to increase at 520 K, when the alloy is still fully amorphous.
- 2 the nucleation rate of the AP2 material is much higher than that of the AP1.
- 3 differences in morphology, spherulitica for AP1 and polygonal for AP2 material.
- 4 in II stage, after the onset of crystallization  $d_{AM}$  remains constant for AP1 and changes for AP2 material.

#### 3.4 SEM with X-Ray Energy Dispersive Analysis.

The cross-section of AQ, AP1 and AP2 ribbons has been analyzed for variation in Fe and Si content. No variations in composition were encountered over a large number of spot analyses for either AQ or AP1 ribbon, however, this was not the case for AP2. On the basis of analyses of several different lengths of ribbon calculations confirm that:

- 1 the iron content for AP2 material showed a  $\pm 10\%$  variation from the average value obtained for the sample.
- 2 the silicon content varied about  $\pm 16\%$  from the average value for AP2 material.
- 3 when the results obtained for AQ and AP1 materials were compared no significant differences in composition were detected for iron or silicon.

#### 4 DISCUSSION

Since the existence of the spin glass state and its magnetic properties

depends mainly on the iron content [10], it follows that the distances between Ni-Fe and Fe-Fe atoms are very important structural factors. Therefore any changes of free volume, as well as development in chemical short-range order (CSRO), which occurs during the relaxation process, must considerably affect the low temperature magnetic properties of the spin glass. The results described in part 3 exhibit interesting features of the short range order (SRO) transformations in the amorphous state. These results confirm the mechanism of the two stage relaxation process proposed by Van den Beukel and Radelaar [11], which suggests the annihilation of excess free volume in the first stage and the regroupments of atoms in SRO in the second stage of relaxation.

The first annealing process AP1 produced a significant increase in density, an increase in the thermal stability i.e. an increase in  $E_a$ , by 10% and slight tendency for an increase in  $T_{x1}$  which is particularly noticeable at low heating rates. However, the crystallization mechanism, nucleation rate and morphology of the first crystals to appear remained unchanged for both AQ and AP1 materials. The SEM results confirmed the similarity of AQ and AP1 specimens with respect to local variation in composition.

During the annealing process AP1 the first stage of relaxations was attained. According to Graham and Egami [12] relaxation is characterized by the elimination of excess free volume and the annihilation or transformation of large unstable defects to smaller more stable defects. By using mechanisms from both of the above papers i.e. the two stage relaxation and transformation of defects a satisfactory explanation of our results can be made. A constant value of  $d_{AM}$  was obtained for the AP1 material up to 520 K followed by an increase

above that temperature, and this seems to indicate there is a thermal activation threshold resulting from the transformation to the smaller but more stable defects proposed by Graham and Egami. This mechanism does not operate in the AP2 material, because during the higher temperature annealing process the defect transformation has been completed. A regroupment of iron and metalloid atoms has been produced during the AP2 annealing process, and has accordingly altered the CSRD by forming areas of high iron and metalloid atom concentrations. Furthermore, the probability of an increase in Fe-Fe pairs is likely and this would obviously affect the magnetic properties at low temperature. The structure still remains fully amorphous and shows higher thermal stability, exhibited by the fact that the value of  $d_{AM}$  remains unchanged until 680 K. Also the nucleation rate for AP2 is much higher than for the AP1 material, and a resulting morphology difference confirms the existence of a much larger number of nucleation sites in the AP2 material.

Metal<sub>3</sub> metalloid clusters in the amorphous phase were proposed by Piller and Haasen [13] and applied by Zielinski [9] for an interpretation of the relaxation mechanism for (Fe,Ni)<sub>80</sub>(B,Si)<sub>20</sub> alloys. It may be assumed that clusters are formed during the AP2 process, and for this alloy composition the most probable resulting structure is that of the metal<sub>3</sub> metalloid. If the clusters are considered to be nucleation sites it follows that there would be an increase in the nucleation rate. Also a regroupment of atoms to form clusters produces a more favourable energy condition within the alloy, and therefore, an increase in thermal stability, i.e. an increase in  $E_{a1}$  and  $T_{x1}$ .

A number of papers have appeared reporting metal-metalloid bonding interaction for most metal-metalloid multicomponent glasses [14,15,16].

When the results of these works were fitted to those of the alloy in this investigation the most probable structure of the clusters the AP2 material was found to be  $\text{Ni}_3\text{B}$  although  $\text{FeNi}_2\text{B}$  cannot be completely excluded. To support this finding, electron diffraction patterns were measured and these results confirmed that the first crystals appear correspond to the  $\text{Ni}_3\text{B}$  phase. It would, therefore, appear these crystals have developed from clusters of a similar structure composition. The formation of such clusters is further substantiated by the results of Vincze et al. [17] and Walter [18], where it has been shown that preferential bonding takes place between nickel and boron atoms.

In the investigation of spin glasses by Rao and Chen [19] and Crook et al. [20] it was pointed out that the spin glass temperature  $T_f$ , the Curie temperature,  $T_c$  are both functions of the density of the magnetic atoms. Tentative measurements of susceptibility have been carried out on  $\text{Fe}_{10}\text{Ni}_{65}\text{B}_{15}\text{Si}_{10}$  ribbon (not reported in this paper) and the results show that the annealing process has a definite effect on this parameter. Namely, the  $T_f$  temperature remains constant within experimental limits for materials AQ and AP1 and there is a slight increase in the value for AP2. It, therefore, seems reasonable to assume that the spin glass transformation also depends on the particular positions taken up by the magnetic atoms i.e. on the relaxation state of the alloy.



### SUMMARY

The object of this research was to exhibit how annealing and the resulting relaxation, affects the amorphous structure of spin glass, after two different heat treatments.

Experimentally, two annealing temperatures and times were chosen to produce two different types of CSRO and still maintain an amorphous structure. Clustering was also described, as well as its effect on the early stages of the crystallization process.

The results of this work should be useful in explaining the changes in magnetic properties, transition temperature,  $T_f$  and Curie temperature,  $T_c$  for various relaxation states in spin glass.

### ACKNOWLEDGEMENTS

The research was sponsored by USAF Grant No AFOSR-80-0005 and this support is gratefully acknowledged.

## REFERENCES

1. P.A. Beck, in "Magnetism in Alloys", ISM-AIME, New York, 1972
2. J.L. Tholence, R. Tournier, J. Phys. Colloq. 35, 229 (1974)
3. I. Reiss, Commum. Phys. 2, 37 (1977)
4. U. Larsen, Phys. Rev. B 14, 4356 (1976)
5. S.F. Edwards, P.W. Anderson, J. Phys. F 5, 965 (1976)
6. D. Sherrington, S. Kirkpatrick, Phys.Rev.Lett. 35, 1792 (1975)
7. C.M. Soukoulis, K. Levin, Phys.Rev. B 18, 1439 (1978)
8. for example M.G. Karkut, R.R. Hake, Proc. 5th Liquid and Amorphous Metals Conf. Los Angeles 1983, J. Non-Cryst. Solids 61 & 62, 595 (1984)
9. P.G. Zielinski, D.G. Ast, Proc 5th Liquid and Amorphous Metals Conf. Los Angeles, 1983, J. Non-Cryst. Solids 61 & 62, 1021 (1984)
10. T. Kudo, T. Egami, J. Appl. Phys. 53, 2214 (1982)
11. A. Van den Beukel, S. Radelaar, Acta Metall. 31, 419 (1983)
12. C.D. Graham, T. Egami, Ann.Rev.Mater.Sci. 8, 423 (1978)
13. J. Piller, P. Haasen, Acta Metall. 30, 1 (1982)
14. H.S. Chen, Acta Metall, 22, 897 (1974)
15. W.L. Johnson, A.R. Williams, Phys. Rev. B20, 1640 (1979)
16. R.P. Messmer, Phys. Rev. B23, 1616 (1981)
17. I. Vincze, D.S. Boudreaux, M. Tegze, Phys.Rev.B 19, 4896 (1979)
18. J.L. Walter, J.Mater.Sci.Eng. 39, 95 (1979)
19. K.V. Rao, H.S. Chen. Proc. 4th Rapidly Quenched Metals Conf., Japan Institute of Metals, Sendai 1981. vol II. p.1073
20. R. Crook, E.D. Dahlberg, K.V. Rao, Proc. 5th Rapidly Quenched Metals Conf. Wuerzburg. 1984, paper G33

### Captions of Figures

Fig. 1. DSC thermogram at heating rate  $20 \text{ K min}^{-1}$

Fig. 2. Bend test plot of interplaten distance  $l$  vs normalised pressure  $\sigma$ ;  $l_0$ -beginning of permanent deformation,  $t$ -ribbon thickness,  $\epsilon$ -strain,  $\epsilon = t/(l-t)$ .

Fig. 3. Stages of the in-situ crystallization of AP1 material. Ia-DP at 520 K (a); II-morphology and DP at 720 K (b,c); III-BF and DP after annealing at 730 K for 15 min. (d,e).

Fig. 4. Stages of the in-situ crystallization of AP2 material; I-DP at 680 K (a); II-DP at 730 K (b); III-morphology DF and DP at 740 K (c,d)

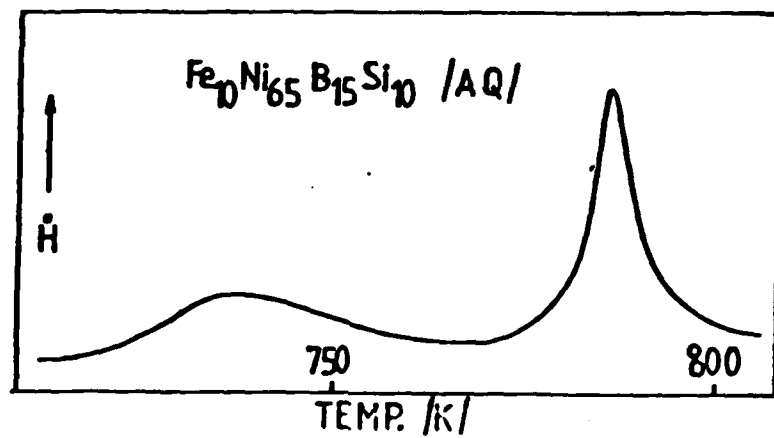


Figure 1

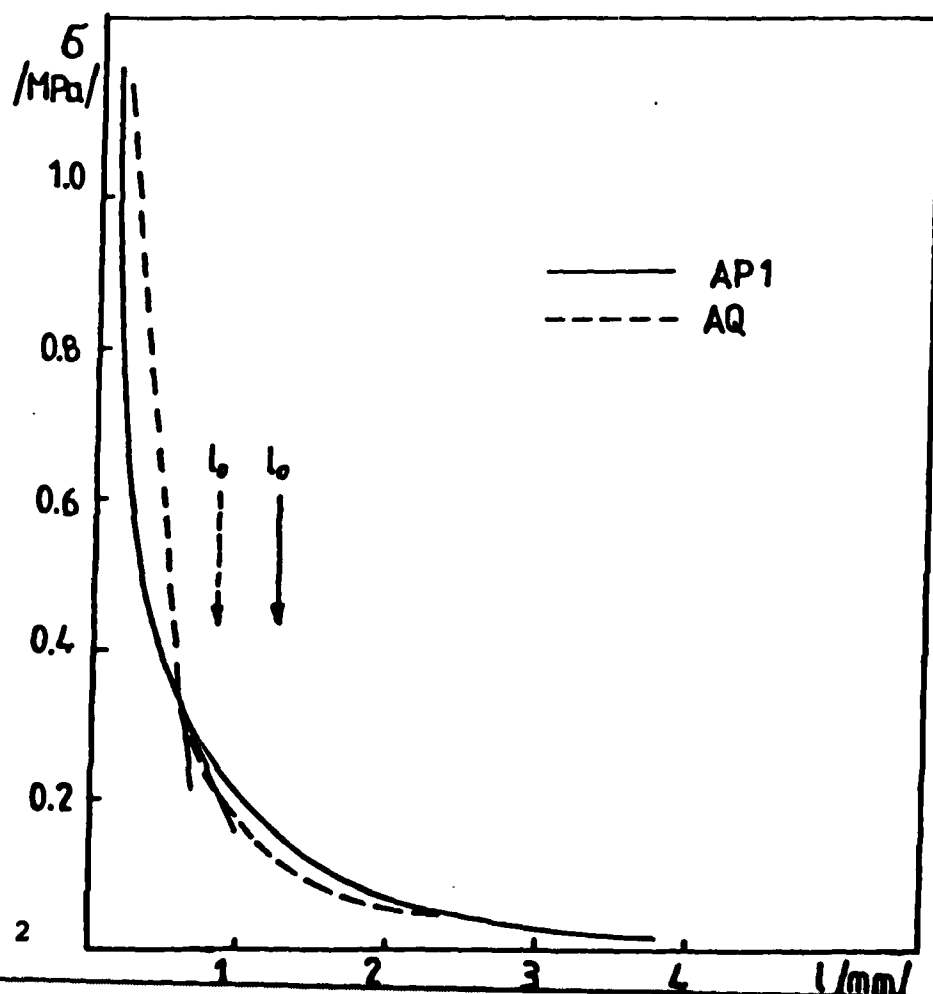


Figure 2

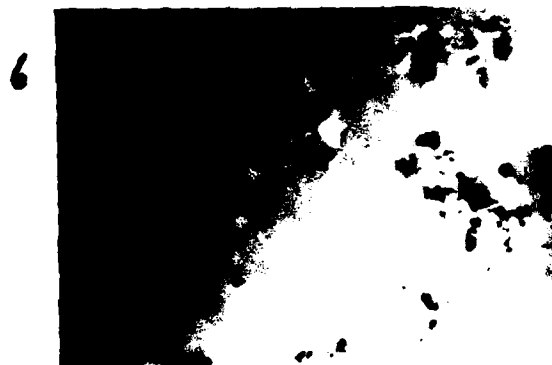
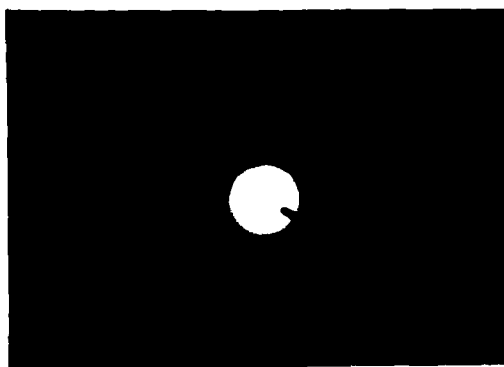


Fig. 3

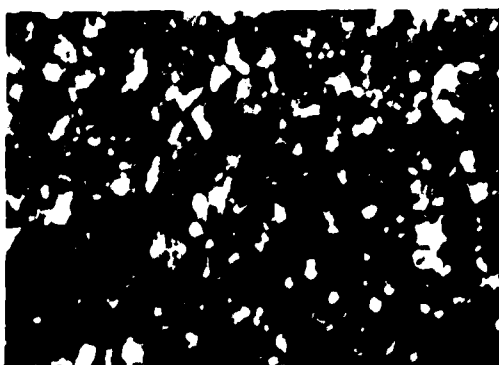
a



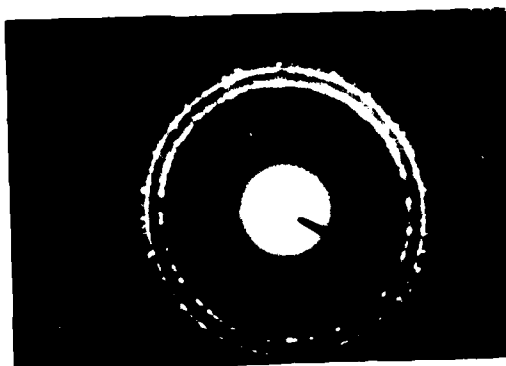
b



c



d



### CONFERENCES

1. MMM Conference, Pittsburgh, 1983
2. 5th RAPIDLY QUENCHED METALS, Wuerzburg (FRG), 1984
3. Meeting on Rapidly Solidified Alloys, Sheffield (I.K.) 1983
4. M.M.M. Conference, San Diego 1984

### PAPERS

1. A.J. JANICKI, Crystallization of  $\text{Ni}_{60}\text{Hf}_{40}$  Amorphous Alloy, 5th Rapidly Quenched Metals Conf., Wuerzburg (FRG) 1984 paper B58.
2. P.J. GRUNDY, S.F. PARKER, A.J. JANICKI, Property Changes in Irradiated Metallic Glasses, Meeting on Rapidly Solidified Alloys, Sheffield (U.K.) 1983
3. A.J. JANICKI, C.A. FAUNCE, R.S. TEBBLE, Relaxation Process of  $\text{FeNiBSi}$  Amorphous Alloy, to be published.
4. A.J. JANICKI, P.J. GRUNDY, R.S. TEBBLE, Crystal structures of Co-Ga spin glass alloys, to be published.

**END**

**FILMED**

**2-85**

**DTIC**











